SIMULATION & DESIGN OF POWER FACTOR CORRECTION PROTOTYPE FOR BLDC MOTOR CONTROL

Pradeep Kumar, B.E., M.Tech.

Electronics Engineering Department, YMCA University of Science and Technology, Faridabad, Haryana, INDIA

P.R.Sharma, B.Tech., M.Tech., PhD

Electrical Engineering Department, YMCA University of Science and Technology, Faridabad, Haryana, INDIA,

Ashok Kumar, B.Tech., M.Tech., PhD

M.R. International University, Faridabad, Haryana, INDIA

Abstract

This paper presents a design, development and simulation of a controller prototype for Power Factor Correction circuit applied to BLDC Motor Control. A laboratory prototype model of the Power Factor Correction circuit is designed and fabricated. Mathematical modelling and simulation of the power factor correction circuit are implemented on the MATLAB Simulink. The control algorithm is implemented on a 16 bit microcontroller dsPIC33FJ32MC204 from Microchip. Experimental results thus obtained on the prototype are also reported in the paper.

Keywords: *BLDC, PFC, Energy Efficiency, AC-DC Converters, DC-DC Converters, THD*

Introduction

There is a lot of interest in using Brushless DC (BLDC) motors now days as it offers so many advantages as compared to the DC motor. Among the numerous advantages of a BLDC motor over a brushed DC motor are absence of the mechanical commutator which allows higher speeds. Brush performance also limits the transient response in case of DC motor. Source of heating in the BLDC motor is the stator, while in the DC motor it is the rotor, therefore it is easier to dissipate heat in the BLDC and reduce audible and

electromagnetic noise (Chia-Hao Wu & Ying-Yu Tzou, 2009, Ozturk, S.B &Oh Yang; Toliyat, H.A. 2007).

There are many different types of brushless motors, and the differences are: the number of phases in the stator, the number of poles in the rotor, the position of the rotor and stator relative to each other (rotor spinning inside the stator vs. rotor spinning outside the stator (Vinaya Skanda)

However all these advantages come with a price. As electronic commutation is applied in control of BLDC motor, complexity of Power Electronic circuit is increased. To achieve accurate and better performance from a BLDC motor, it is generally fed from a Voltage Source Inverter (VSI). In this paper a MOSFET based 3Φ Voltage Source Inverter is proposed. Use of VSI for controlling the BLDC also contributes to increase in Total Harmonics Distortion (THD) of input current. The scheme proposed in this paper provides a simple yet cost effective strategy to reduce the harmonics and achieve near unity Power Factor.

Mathematical Modelling Of Brushless Dc (BLDC) Motor

The three phase star connected BLDC can be modelled by following equations:

$$v_{ab} = R(i_a - i_b) + L\frac{d}{dt}((i_a - i_b) + e_a - e_b \quad (1)$$

$$v_{bc} = R(i_b - i_c) + L\frac{d}{dt}(i_b - i_c) + e_b - e_c \quad (2)$$

$$v_{ca} = R(i_c - i_a) + L\frac{d}{dt}(i_c - i_a) + e_c - e_a \quad (3)$$

$$T_e = k_f \omega_m + J\frac{d\omega_m}{dt} + T_L \quad (4)$$

v, i and e are voltage phase to phase, phase current and phase back e.m.f. respectively. L and R are per phase inductance and resistance respectively, whereas Te and T_L are electrical and load torque respectively. Because of three phase balanced system back e.m.f of the BLDC for each phase can be described:

$$e_a = \frac{k_e}{2}\omega_m F(\theta_e) \quad (5)$$

$$e_b = \frac{k_e}{2}\omega_m F\left(\theta_e - \frac{2\pi}{3}\right) \quad (6)$$

$$e_c = \frac{k_e}{2}\omega_m F\left(\theta_e - \frac{4\pi}{3}\right) \quad (7)$$

$$T_e = \frac{k_t}{2}\lfloor F(\theta_e) i_a \rfloor + \left\lfloor F\left(\theta_e - \frac{2\pi}{3}\right) i_b \right\rfloor + \left\lfloor F\left(\theta_e - \frac{4\pi}{3}\right) i_c \right\rfloor \quad (8)$$

k_e and k_t are the constant of back emf and torque respectively Based on equation (1), (2) and (3) it is evident that each voltage is a linear combination of other two voltages. Two equations are sufficient for deriving the mathematical model.

So from eqn (1), (2), (4) a complete model can be written as:

$$\begin{pmatrix} i_a' \\ i_b' \\ \omega_m' \\ \theta_m' \end{pmatrix} = \begin{pmatrix} -\frac{R}{L} & 0 & 0 & 0 \\ 0 & -\frac{R}{L} & 0 & 0 \\ 0 & 0 & -\frac{k_f}{J} & 0 \\ 0 & 0 & 1 & 0 \end{pmatrix} \begin{pmatrix} i_a \\ i_b \\ \omega_m \\ \theta_m \end{pmatrix} \qquad 9$$

Translating equation (5),(6),(7) and (9) into simulink model gives following BLDC model as depicted in Fig.1.

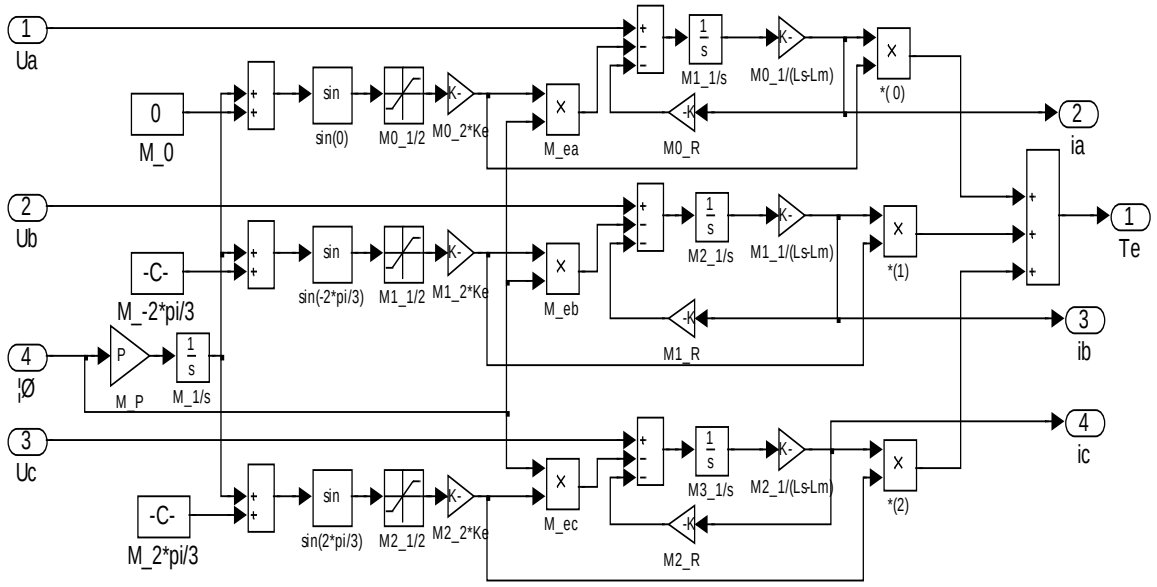

Fig.1: Simulation model of the BLDC

Working Of A Brushless Dc (BLDC) Motor

In order to run a BLDC motor, a rotating Electric Field is necessary. A three-phase BLDC motor has three Stator phases out of which two are excited at a time to create a rotating electric field. This method is fairly easy to implement, but to prevent the permanent magnet rotor from getting locked with the stator; the excitation sequence must be applied in a specific manner while knowing the exact position of the rotor magnets. Position information can be gotten by either a shaft encoder or, more often, by Hall Effect sensors that detect the rotor magnet position. In a typical three phase, sensored BLDC motor there are six distinct regions or sectors in which two specific windings are excited. Commutation sequence of a three phase BLDC is depicted in fig. 2.

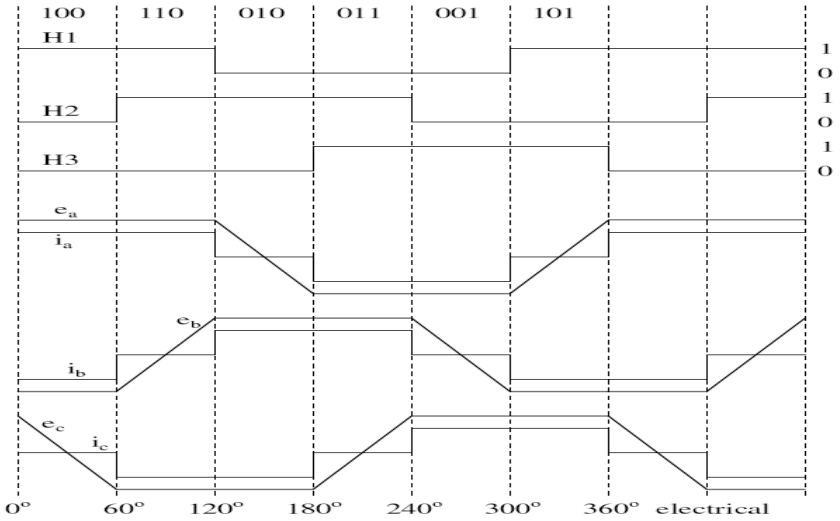

Each commutation sequence has one of the windings energized with positive power (current enters into the winding), the second winding is negative (current exits the winding) and the third is in a non-energized condition. Torque is produced because of the interaction between the magnetic field generated by the stator coils and the permanent magnets. Ideally, the peak torque occurs when these two fields are at 90° to each other and falls off as the fields move together. In order to keep the motor running, the magnetic field produced by the windings should shift position, as the rotor moves to catch up with the stator field. What is known as “Six-Step Commutation” defines the sequence of energizing the windings.

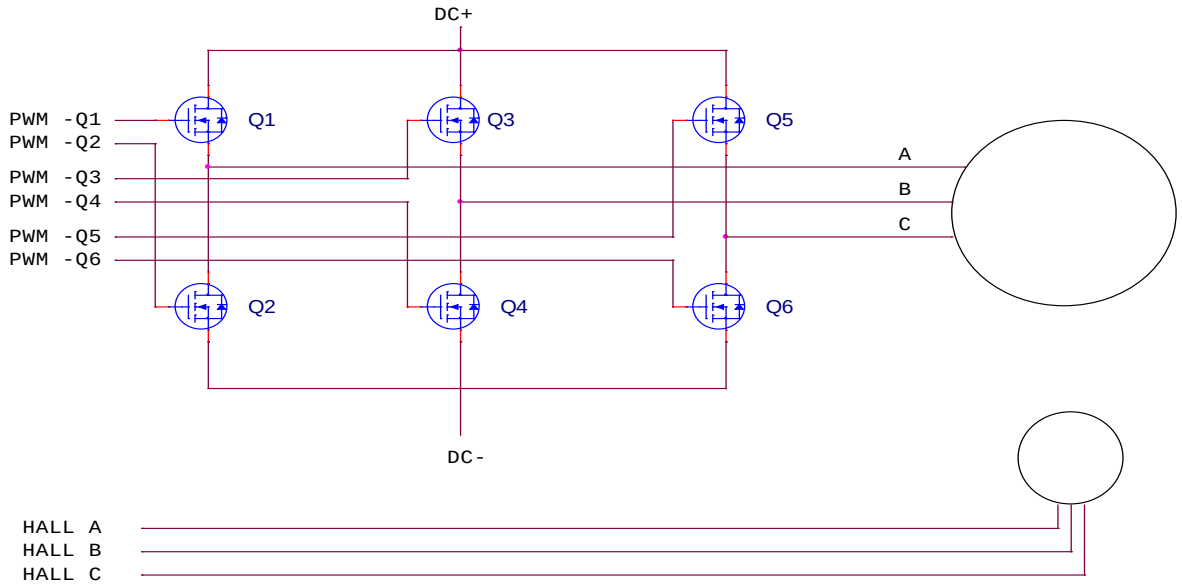

Fig.3 Schematic of BLDC Control

Table 1 - Sequence For Rotating The Motor In Clockwise Direction

Sequen	Hall Sensor Input			Active PWM		Phase Current		
	A	B	C			A	B	C
1	0	0	1	Q1	Q6	DC+	OFF	DC-
2	0	0	0	Q1	Q4	DC+	DC-	OFF
3	1	0	0	Q5	Q4	OFF	DC-	DC+
4	1	1	0	Q5	Q2	DC-	OFF	DC+
5	1	1	1	Q3	Q2	DC-	DC+	OFF
6	0	1	1	Q3	Q6	OFF	DC+	DC-

Table 2 - Sequence For Rotating The Motor In Anti Clockwise Direction

Seq uen	Hall Sensor Input			Active PWM		Phase Current		
	A	B	C			A	B	C
1	0	1	1	Q5	Q6	OFF	DC-	DC+
2	1	1	1	Q1	Q4	DC+	DC-	OFF
3	1	1	0	Q1	Q4	DC+	OFF	DC+
4	1	0	0	Q3	Q2	OFF	DC+	DC+
5	0	0	0	Q3	Q2	DC-	DC+	OFF
6	0	0	1	Q5	Q6	DC-	OFF	DC+

By reading the Hall effect sensors, a 3-bit code can be obtained with values ranging from 1 to 6 as shown in figure . Each code value represents a sector on which the rotor is presently located. Each code value, therefore, gives us information on which windings need to be excited. Thus a simple lookup table can be used by the program to determine which two specific windings to excite and, thus, turn the rotor.

Power Factor Controller Design

The Controller of the PFC consists of two control loops –one for voltage control and another for current control. Two PI controller one for Voltage and another for current are implemented. Voltage Controller loop continuously scan reference dc voltage compares the same with actual dc output voltage (Pradeep Kumar, P. R. Sharma and Ashok Kumar 2012). The error is processed through a PI controller and a current reference is generated by multiplying the input AC Voltage.

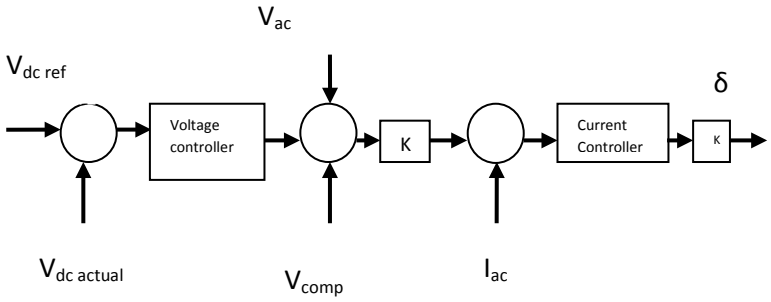

Fig.4 Controller Block Diagram for PFC

The current reference acts as a reference to inner current controller loop, which produces the duty ratio information for the PWM pulses.

Transfer function of the Voltage Controller is given by

$$G_V(s) = k_{pv} + \frac{k_{iv}}{s} \qquad 10$$

Where k_{pv} is proportional constant for voltage controller and k_{iv} is the integral constant for voltage controller

$$G_v(s) = k_{pv}\left(\frac{1+Ts}{Ts}\right) \qquad 11$$

Similarly Transfer function of the current Controller is given by

$$G_i(s) = k_{pi} + \frac{k_{ii}}{s} \qquad 12$$

Voltage controller bandwidth is 10 Hz, so that the 2nd harmonic ripple in the DC bus voltage are eliminated

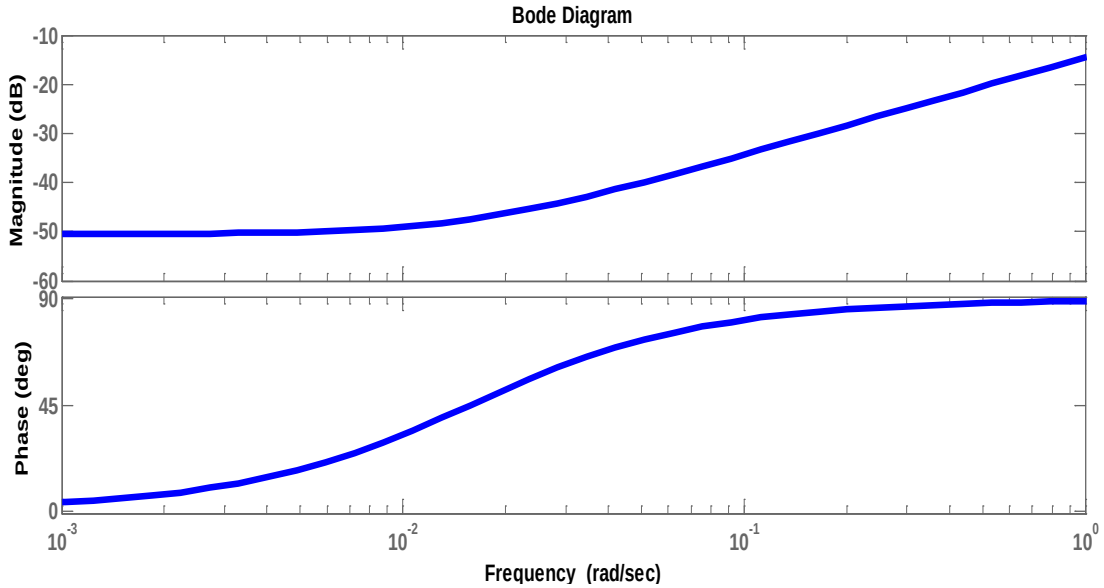

Fig.5 Bode plot of designed voltage controller

Considering the Bandwidth of the controller 10 KHz for faithfully tracking the rectified voltage of the frequency of 100 Hz. Location of zero is chosen to be 800 Hz well below 8 KHz, the cross over frequency of 8 KHz. for the Current controller.

$$G_i(s) = k_{pi}\left(\frac{1+Ts}{Ts}\right) \qquad 13$$

Where k_{pi} is proportional constant for current controller and k_{ii} is the integral constant for current controller.

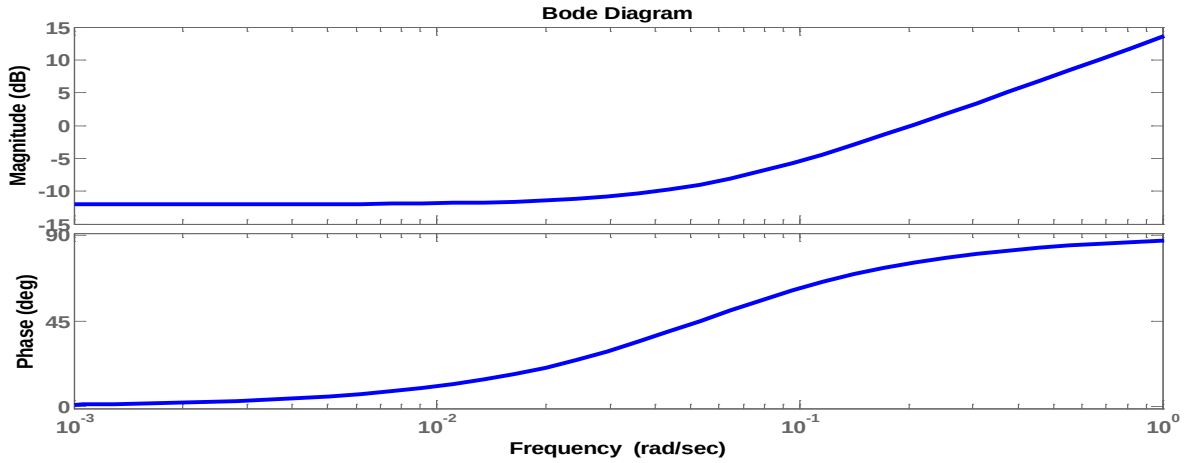

Fig.6 Bode plot of designed current controller

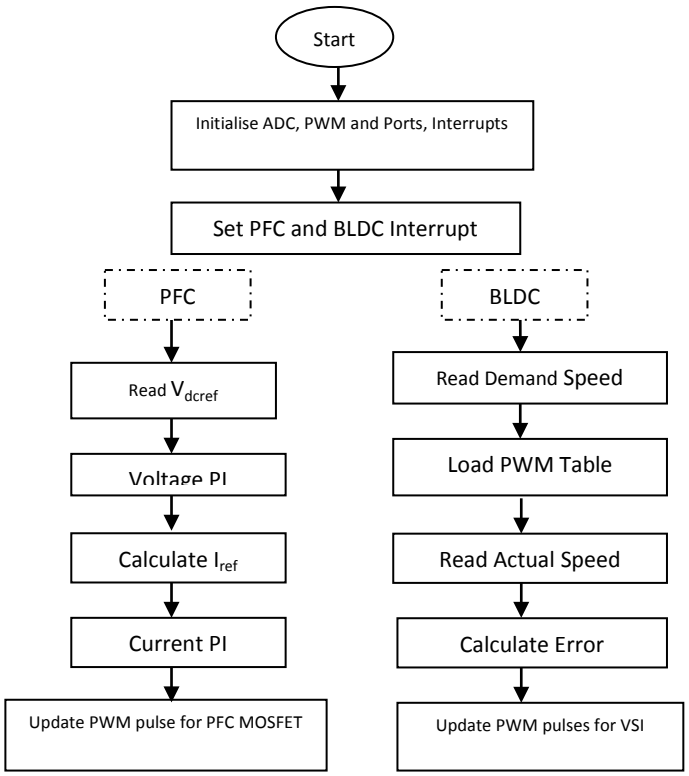

Fig. 7 Flow Chart for the software of the Power Factor Correction for BLDC

Software of the controller as depicted in Fig.7 is implemented on dsPIC. There are two interrupt initialised for operating Power Factor Correction.

Design Of A Power Factor Correction Prototype For Bldc

Figure depicts the prototype developed to demonstrate the implementation of a Power Factor Correction for a BLDC Motor. 1st stage of the prototype consists of a Boost converter, followed by a 3 Φ MOSFET inverter. Boost converter is realised by a an advanced smart power module FPAB30BH60 developed by Fairchild Semiconductor. It is a combination of protection circuitry and drive IC matched to high frequency switching IGBTs (Smart Power Module Data sheet) There is also a provision integrated under-voltage lock-out and over-current protection function. Internal block diagram of the module is shown in fig.8.

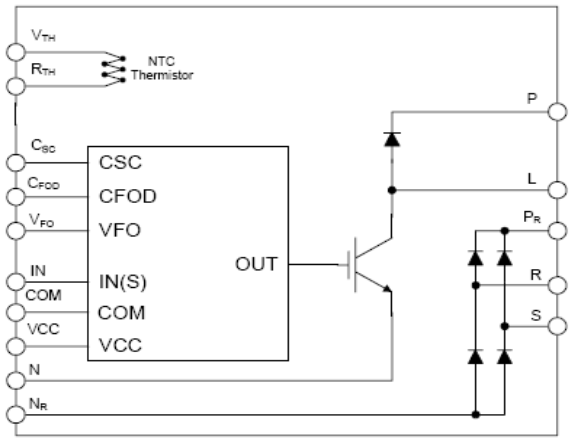

Fig. 8 : Internal Equivalent Circuit of FPAB30BH60

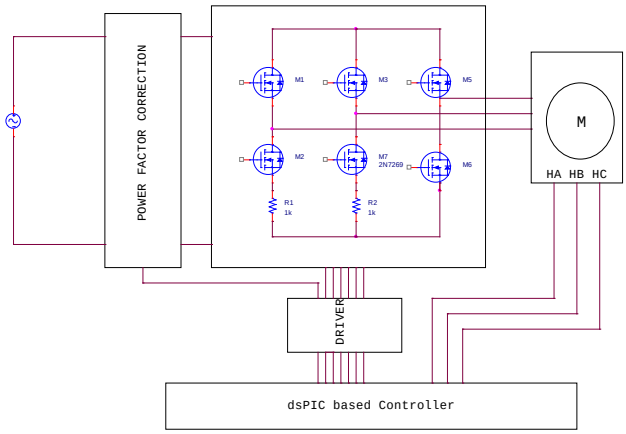

Fig. 9: Schematic of the PFC for BLDC

Simulation Results

Simulations carried out on MATLAB are reported as below:

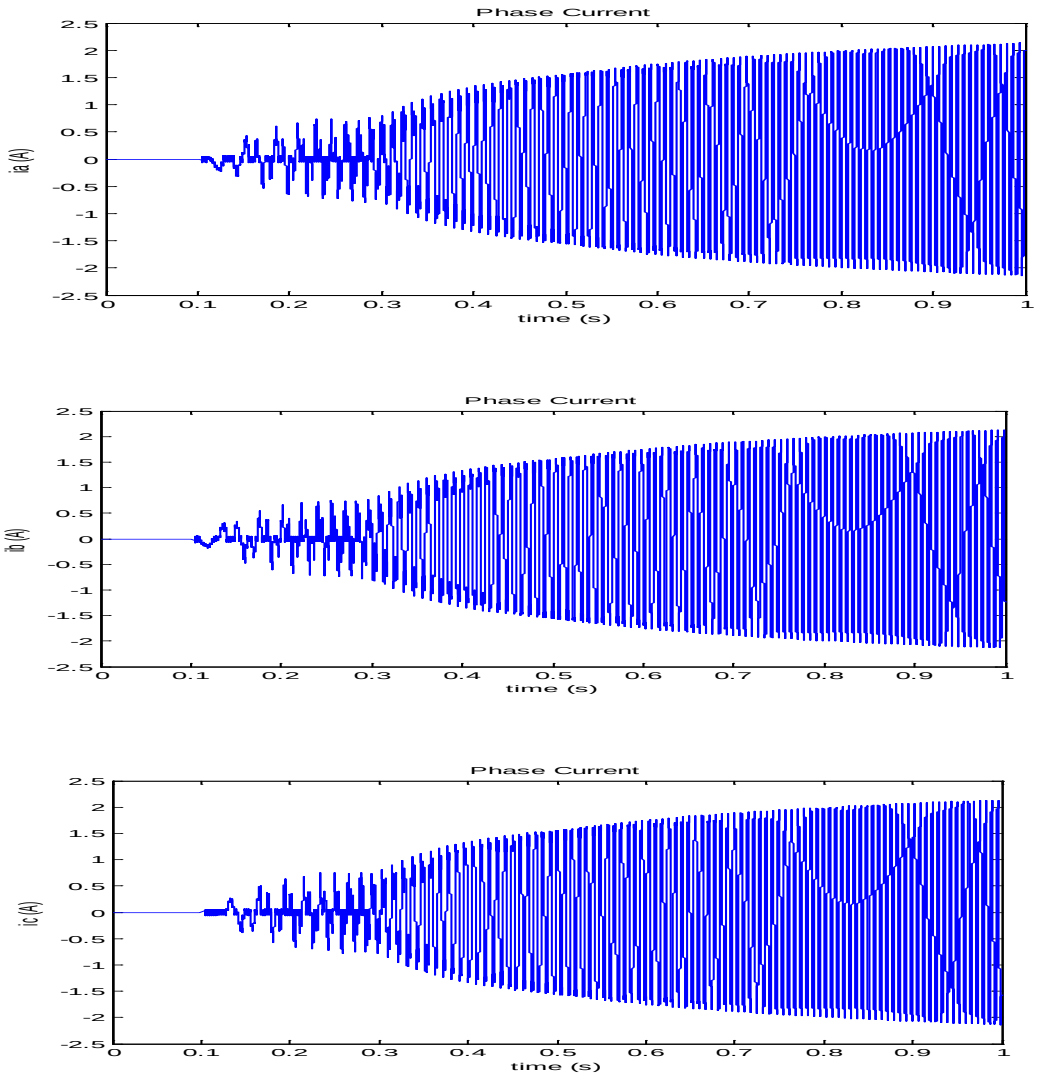

Fig. 10 (a), (b) and (c) : Phase Currents of the Simulated BLDC Controller

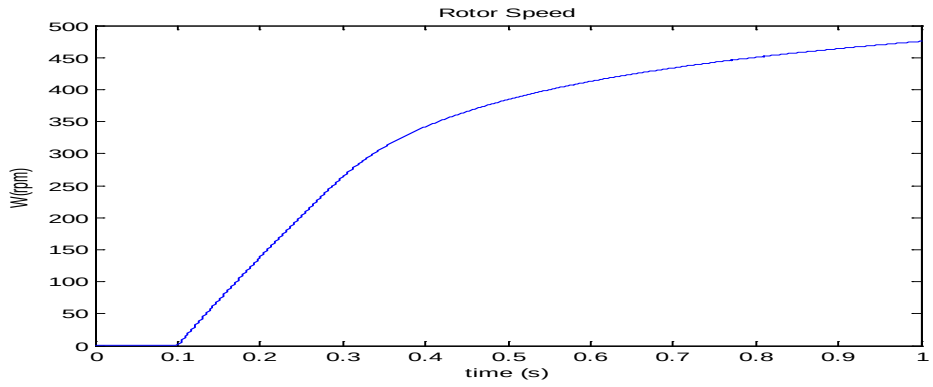

Fig. 11: Simulated BLDC Controller Rotor Speed

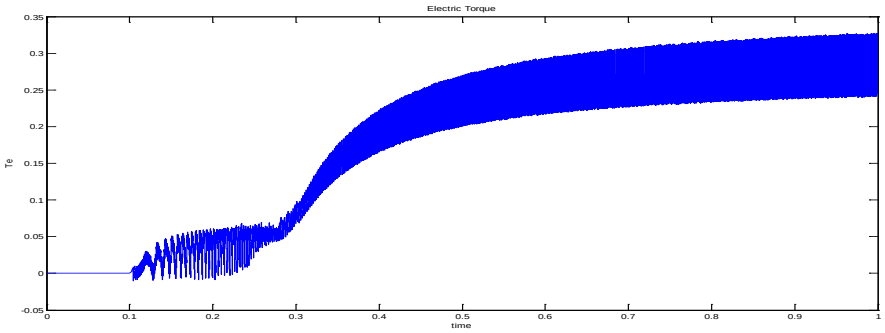

Fig. 12: Simulated BLDC Controller Electric Torque

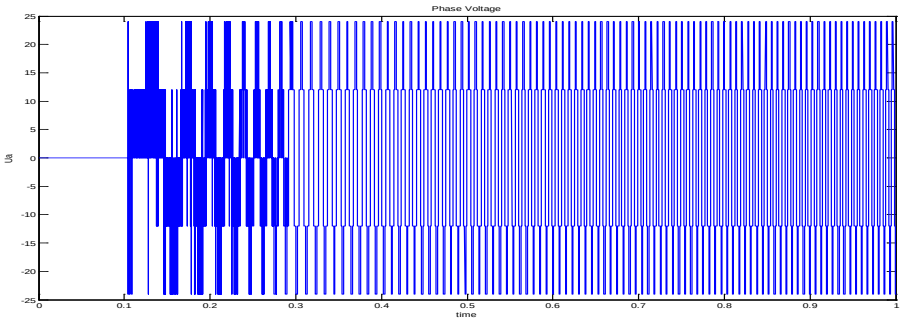

Fig. 13: Simulated BLDC Controller Phase Voltage

All the simulation results are obtained on the MATLAB simulink for a step load demand varied from 0 to 0.3 mNm.

Experimental results

Experimental Results as obtained from the prototype developed are as following:

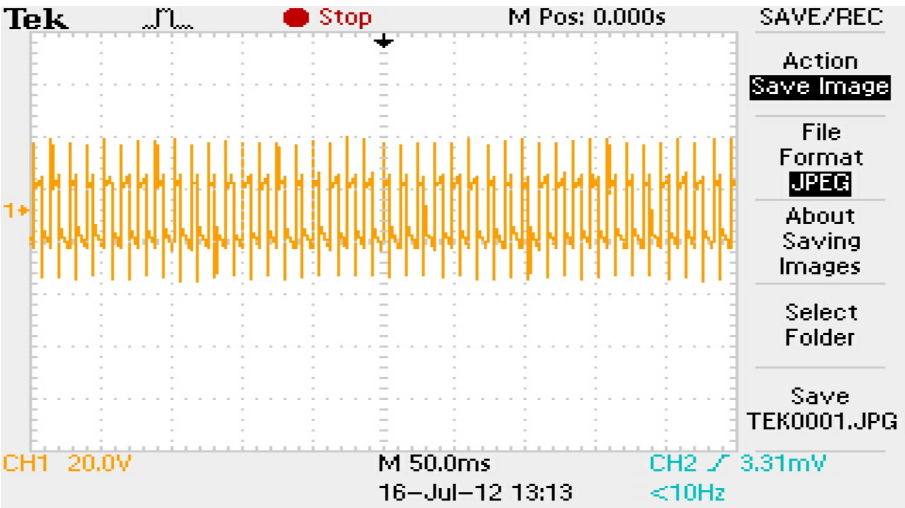

Fig.14. Line Voltage of BLDC

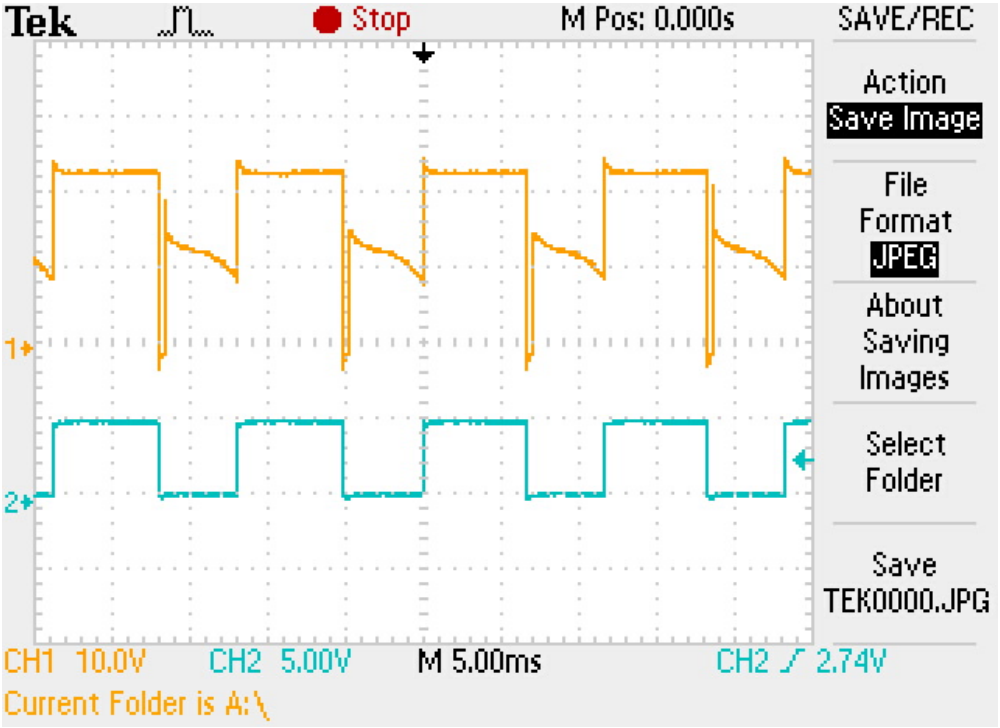

Fig.15: Phase Voltage and corresponding Hall Sensor output

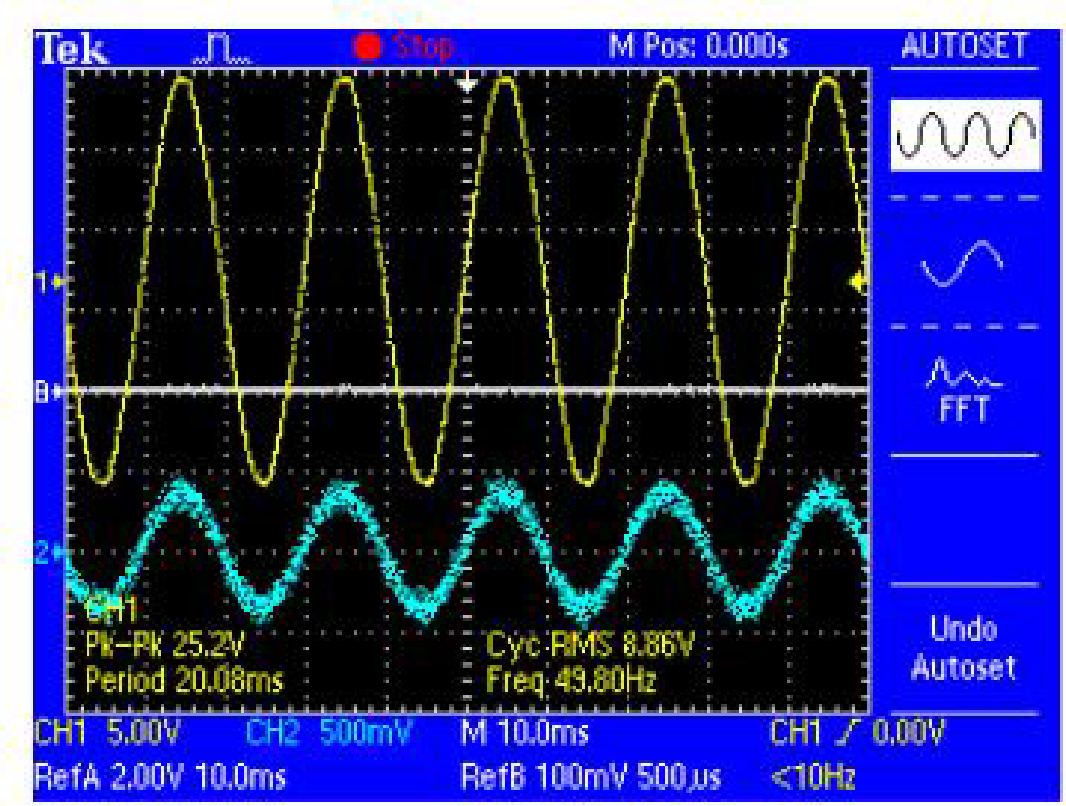

Fig.16: Input Voltage and current with PFC

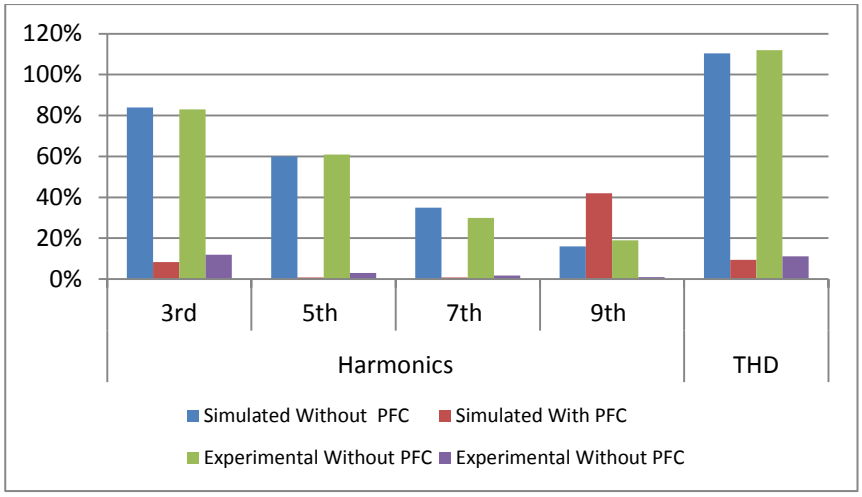

Fig. 17: Comparison of Simulated and actual Harmonic and THD

Conclusion

An overview of the Power Factor Correction for BLDC motor is presented. Implementation of the PFC on a microcontroller is achieved. It shows that a low cost solution for Power Factor Correction as applied to BLDC motor control is workable and cost effective.

References:

Chia-Hao Wu; Ying-Yu Tzou," Digital control strategy for efficiency optimization of a BLDC motor driver with VOPFC" Energy Conversion Congress and Exposition, 2009. ECCE 2009. IEEE pp: 2528 - 2534

Ozturk, S.B.; Oh Yang; Toliyat, H.A.,"Power Factor Correction of Direct Torque Controlled Brushless DC Motor Drive" Industry Applications Conference, 2007. 42nd IAS Annual Meeting. Conference Record of the 2007 IEEE 2007 , pp: 297 – 304

Hongmei Yang; Hua Gua; Xin Yu,"Design of brushless DC motor control system based on DSP" Qingqing Zhang , 2012 2nd International Conference on Consumer Electronics,, Page(s): 3195 – 3198

R.Loera-Palomo, J.A. Morales- Saldana, J.Leyva-Ramos, E.E.Carbajal – Gutierrez "Controller Design for a Power Factor Correction Regulator R2P2 " IET Electron., 2010, vol. 3 Iss.5 pp. 784-792.

Chia-An Yeh, Kung-Min Ho, Yen-Shin Lai, Fumikazu Takashi, Masahiro Hamaogi " Digital Controlled Power Factor with Transition Current Mode Control without Zero Current Detection" pp 198-203, PEDS2009.

R.Balamurugan and Dr.G.Gurusamy: Harmonic Optimization by Single Phase Improved Power Quality AC-DC Power Factor Corrected Converters: pp.46-53, 2010 International Journal of Computer Application Volume 1- No.5.

V.M.Lopez, F.J.Diaz, Ade Castro" Auto tuning Digital Controller for Current Sensorless Power Factor Corrector Stage in Continuous Conduction Mode"@2010 IEEE.

Chung-Wen Hung, Jhih-Han Chen, Li-Sheng Chang, Cheng-Han Li:"A Simple Strategy of Power Factor Correction based on Low- End MCU" pp1229-1233, 5th IEEE Conference on Industrial Electronics and Applications.

Pradeep kumar, P.R.Sharma, Ashok Kumar," Design of a Microcontroller Based PFC" International Journal of Power System Operation and Energy Management ISSN (PRINT): 2231 – 4407, Volume-1, Issue-4, 2012.

C M Bhatia, M S Rao, Pradeep Kumar & Amit Khare; Intelligent Computer Control of Flexible AC Transmission System (FACTS); Journal of IETE, vol 41, no 2; pp 135-141; March - April 1995.

C M Bhatia, M S Rao, P Kumar & Amit Khare; Microprocessor based closed loop laboratory model for Rapid Impedance Control as applied to Flexible AC Transmission System (FACTS); 6th European Conference on Power Electronics and Applications (EPE-95); 18-21 September 1995; Spain.

Pradeep Kumar, P. R. Sharma and Ashok Kumar; Power Factor Correction Based on RISC Controller; Communications in Computer and Information Science, 1, Volume 148, Advances in Power Electronics and Instrumentation Engineering, Part 3, Pages 83-87.

Pradeep Kumar, P. R. Sharma and Ashok Kumar; Power Factor Correction for Low Power Supplies; 5th International Multi Conference o Intelligent Systems, Sustainable, New and Renewable Energy technology 7 Nanotechnology, February 18-20, 20011 (IISN 2011) , Pages GS1- 5.

Power Factor Correction Handbook- ON Semiconductor

Vinaya Skanda".Power Factor Correction in Power Conversion ApplicationsUsing the dsPICDSC" Application note Microchip Technology Inc

Fairchild Semiconductor – Smart Power Module Data sheet.